Research Article

Kenta Yamanaka*, Manami Mori, Kazuo Yoshida, Phacharaphon Tunthawiroon, and Akihiko Chiba

Corrosion behavior of a Co-Cr-Mo-Si alloy in pure Al and Al-Si melt

https://doi.org/10.1515/htmp-2022-0278 received December 17, 2022; accepted May 30, 2023

Abstract: Metallic phase change materials (MPCMs) are attracting considerable attention for their application in thermal energy storage. Al-Si alloys are considered potential MPCMs; however, to develop storage systems/modules, it is crucial to fabricate corrosion-resistant materials for MPCMs. In this study, the corrosion behavior of Co-28Cr-6Mo-1.5Si (wt%) alloy was examined via immersion tests in commercial Al-Si alloy (ADC12) melt at 700°C for 10 h. The results were compared to those obtained for pure Al. Substrate thickness loss measurements revealed that the liquid metal corrosion was more severe in the Al -Si melt than that in pure Al, suggesting an increased reactivity due to Si addition. Interfacial analysis elucidated a direct reaction between the alloy substrate and molten Al in both cases. Furthermore, the formation of oxides such as Al₂O₃ and SiO₂ did not contribute to corrosion resistance.

Keywords: phase change material, aluminum, corrosion, Co–Cr–Mo alloys

Phacharaphon Tunthawiroon: Department of Industrial Engineering, School of Engineering, King Mongkut's Institute of Technology Ladkrabang, Bangkok, 10520, Thailand

Akihiko Chiba: Institute for Materials Research, Tohoku University, 2-1-1 Katahira, Aoba-ku, Sendai 980-8577, Japan

1 Introduction

Substituting fossil fuels with renewable energy sources is a global challenge that is the key to solving future energy problems and developing a sustainable society. Recently, the number of solar power plants has increased because of the decreased cost of photovoltaic panels. However, sunlight is unavailable at night leading to electric power fluctuations. Moreover, the growth of renewable energy sources often causes a mismatch between power supply and demand, which is referred to as "overgeneration" [1]. Therefore, developing power storage technologies is crucial to overcome the "duck curve" in solar power supply, and to create a stable power supply and demand from various energy sources.

Thermal energy storage (TES) is of great interest, as it directly stores the sensible heat or latent heat of storage materials [2]. Phase change materials (PCMs) [3] provide a substantial quantity of heat owing to phase transitions between different states, particularly solid-liquid transitions during charging and discharging. Among the various types of PCMs proposed [3–5], salts are attractive candidates because of their high heat-storage density and suitable melting temperature [6]. However, the low heat conductivity, corrosion activity, large change in volume upon melting, significant overcooling, and costliness of some salts are major drawbacks [6]. Therefore, metallic phase change materials (MPCMs) with relatively high thermal conductivity (~1 to 2 orders of magnitude greater than that of other PCMs) and relatively high volumetric density of energy [7] have received considerable attention. Several alloy systems, such as Mg-Zn, Zn-Al, Al-Mg-Zn, and Al-Si-Cu, have been proposed, and their thermophysical properties have been reported [6]. Among them, Al-Si alloys are suitable heat-storage media because of their high heat of fusion and thermal conductivity [8,9]. Notably, Al-12Si (wt%) alloy, with a composition similar to the eutectic composition in the Al-Si binary phase diagram [10], is commercially available as a cast Al alloy and is considered a cost-effective PCM. However, Al-based alloys

^{*} Corresponding author: Kenta Yamanaka, Institute for Materials Research, Tohoku University, 2-1-1 Katahira, Aoba-ku, Sendai 980-8577, Japan, e-mail: kenta.yamanaka.c5@tohoku.ac.jp Manami Mori: Institute for Materials Research, Tohoku University, 2-1-1 Katahira, Aoba-ku, Sendai 980-8577, Japan; Department of General Engineering, National Institute of Technology, Sendai College, 48 Nodayama, Medeshima-Shiote, Natori 981-1239, Japan Kazuo Yoshida: Institute for Materials Research, Tohoku University, 2-1-1 Katahira, Aoba-ku, Sendai 980-8577, Japan; Eiwa Co., Ltd., 405-45 Kasshi-cho, Kamaishi 026-0001, Japan

are highly corrosive to steels, which are generally used as container materials [11], forming intermetallic compounds such as $FeAl_3$ and Fe_2Al_3 [12,13]. Thus, there is an urgent need to develop technologies and/or materials to mitigate corrosion via interactions between molten Al and containers.

Liquid metal corrosion is a physicochemical process involving the dissolution and transport of species, chemical reactions, and phase transformations [14]. In a previous study, biomedical Co-Cr-Mo alloys, generally used for orthopedic and dental applications [15-17], were examined as potential mold materials for Al die casting [18,19]. A Cr₂O₃ film of Co–29Cr–6Mo (wt%) alloy substrate, which was obtained via a prior isothermal oxidation treatment, was effective in preventing the substrate dissolution by acting as a barrier against attack from molten Al [18]. Moreover, a comparison with the Fe-29Cr-6Mo alloy counterpart indicated the importance of the matrix composition because the formation of Fe₂O₃ in the surface oxide film lowered the corrosion resistance against molten Al [20]. Therefore, AISI H-grade steels containing Cr and Mo, which are utilized for hot work tools and die-casting applications, are easily attacked by molten Al and Al alloys. Some novel steels with improved corrosion resistance in Al melt have been reported [21,22]. Tunthawiroon et al. [19] reported that the addition of Si to the Co-29Cr-6Mo alloy formed a homogeneous Cr₂O₃ film upon isothermal pre-oxidation treatment [23,24], significantly improving the corrosion resistance of the Al melt. Therefore, Co-Cr-Mo-Si alloys are considered potential candidates as container materials in thermal storage systems/modules utilizing Al-Si PCMs. Recently, Yang et al. [25] investigated the corrosion behavior of additively manufactured CoCrWAlx alloys in 6061 Al-Si-Mg alloy at 710-800°C and determined an optimal Al alloying content (2 wt%). However, the effect of adding Si to the Al melt on the corrosion behavior of Co-Cr-Mo-Si alloys has not been thoroughly elucidated. Although the high-temperature corrosion of the containment material is a major challenge in the TES technology [26], the relevant studies have been limited. Sun et al. [27] reported that 304L-grade stainless steel possessed better corrosion resistance in Al-34Mg-6Zn (wt%) alloy than that in the C20 carbon steel, although the difference in the corrosion rate in the melt was not significant. Additionally, the detailed corrosion mechanism was not clear.

In this study, we examined the corrosion behavior of a Co–Cr–Mo–Si alloy in pure Al and commercially available Al–Si alloys at 700°C to reveal the Si alloying effect in the melt. To elucidate the intrinsic corrosion behavior of the alloy, the specimens were not subjected to a pre-oxidation treatment. The results indicated a higher reactivity in

the Al-Si melt and provided fundamental knowledge of the interfacial reaction.

2 Materials and methods

A previous study [19] revealed that the corrosion resistance in a pure Al melt was improved by adding Si to Co–28Cr–6Mo alloys. Therefore, in this study, a Co–28Cr–6Mo alloy containing 1.5 wt% of Si was designed, whereas the Si content for biomedical Co–Cr–Mo alloys (according to the ASTM F1537 standard) was 1 wt% or lower. An ingot weighing approximately 30 kg was prepared via high-frequency vacuum induction melting in Eiwa, Japan. The chemical composition of the alloy is listed in Table 1. The ingot was hot forged after homogenization heat treatment at 1,230°C, followed by solution heat treatment at 1,230°C for 1 h. Hot rolling was performed to produce bars of approximately $50 \times 50 \text{ mm}^2$ in cross-section. Finally, solution heat treatment was conducted at 1,150°C for 30 min in a vacuum, followed by Ar gas cooling.

Samples with a thickness of 3 mm were cut from the bar using electrical discharge machining. The surfaces of the samples were ground with emery paper, followed by polishing with a 1 µm alumina suspension. The immersion tests were conducted in pure Al (99.99 wt%) and Al -Si alloys at 700°C for 10 h. The test temperature, which is above the melting temperature of Al (660°C), is higher than that used for the PCM applications; therefore, these experiments could be regarded as an accelerated test. Table 2 shows the chemical composition of the Al-Si alloy, which is a commercial die-cast alloy (ADC12). Pure Al or ADC12 was placed in an alumina crucible in a muffle furnace. After static immersion tests, the samples were removed and cooled in air. The sample thickness before and after the immersion tests was measured based on the cross-sectional images obtained via optical microscopy (DM2700 M, Leica, Germany). The thickness loss (ΔX) was defined as follows [18]:

$$\Delta X = \frac{X - X_0}{2},\tag{1}$$

Table 1: Chemical composition of the Co-28Cr-6Mo-1.5Si alloy prepared in this study (wt%)

Со	Cr	Мо	Si	Mn	Fe	Ni	С	N
Bal.	27.4	6.17	1.39	0.61	0.11	0.01	0.058	0.18

Table 2: Chemical composition of ADC12 used in this study (wt%)

	Al	Si	Fe	Cu	Mg	Zn	Ti
Measured	Bal.	10.44	0.72	1.88	0.20	0.52	0.15
Standard	Bal.	9.6-12.0	<1.3	1.5-3.5	<0.3	-	-

where X_0 and X represent the sample thickness, before and after immersion, respectively.

Before the immersion tests, the microstructure was characterized using field-emission scanning electron microscopy (FE-SEM; JSM-IT800, JEOL, Japan) at 15 kV. SEM images were acquired in backscatter electron (BSE) mode. Electron backscatter diffraction (EBSD; JSM-IT800, JEOL, Japan) measurements were conducted at 20 kV. Data collection and analysis were performed using OIM Collection/ Analysis software (ver. 7.3, EDAX, USA). The interfaces between Al and the substrate were cut from the immersed samples using a precision cutter (IsoMet LS, Buehler, USA) and examined using a field-emission electron probe microanalyzer (FE-EPMA; JXA-8530 F, JEOL, Japan) at an acceleration voltage of 15 kV. The cross-sections for SEM and EPMA were prepared via mechanical grinding using emery paper (up to #3000, Struers, Japan), polishing with a 0.3 µm alumina suspension (AP-A, Struers, Japan), and mirror-finishing using a 0.04 µm colloidal silica suspension (OP-U, Struers, Japan).

3 Results and discussion

Figure 1 shows the SEM-BSE image, inverse pole figure (IPF) map, and boundary map of the initial microstructure of the Co-28Cr-6Mo-1.5Si alloy substrate before the immersion tests. Equiaxed grains with annealing twins

are observed. The microstructure consists primarily of a face-centered cubic and y phase. The ε phase generally exhibits a plate-like martensite with a hexagonal closepacked structure; however, it is not identified here. EBSD measurements show that the average grain size of the alloy is approximately 100 µm. Although Si addition generally facilitates the formation of intermetallic phases (σ and μ phases) [24,28], negligible precipitates are obtained for 1.5 wt% composition. The corresponding EPMA analysis reveals homogeneous distributions of alloying elements and the presence of some SiO₂ particles (Figure S1). Therefore, the microstructure does not show any significant difference from those obtained in the biomedical-grade alloys (Si content ≤ 1.0 wt%).

Table 3 shows the results of the static immersion tests in pure Al and Al-Si alloy melts at 700°C for 10 h. The thickness losses of the Co-28Cr-6Mo-1.5Si alloy substrates under identical conditions (temperature and duration) were approximately twice as high for the ADC12 melt than for the pure Al counterpart, suggesting that adding Si to the Al melt facilitates the dissolution of the Co-Cr-Mo alloys. Previous studies have demonstrated that the thickness loss of Co-28Cr-6Mo alloys continuously increased with immersion time [18]; however, the corrosion rate decreased with increasing alloyed Si content [19].

Figure 2 shows SEM-BSE images of the Al/substrate interfacial regions. Both images indicate that the dissolution

Table 3: Thickness losses of the Co-28Cr-6Mo-1.5Si alloy substrates in the pure Al and ADC12 melt at 700°C for 10 h

	Thickness loss, $\Delta X~(\mu m)$		
Pure Al	129 ± 19		
ADC12	251 ± 16		

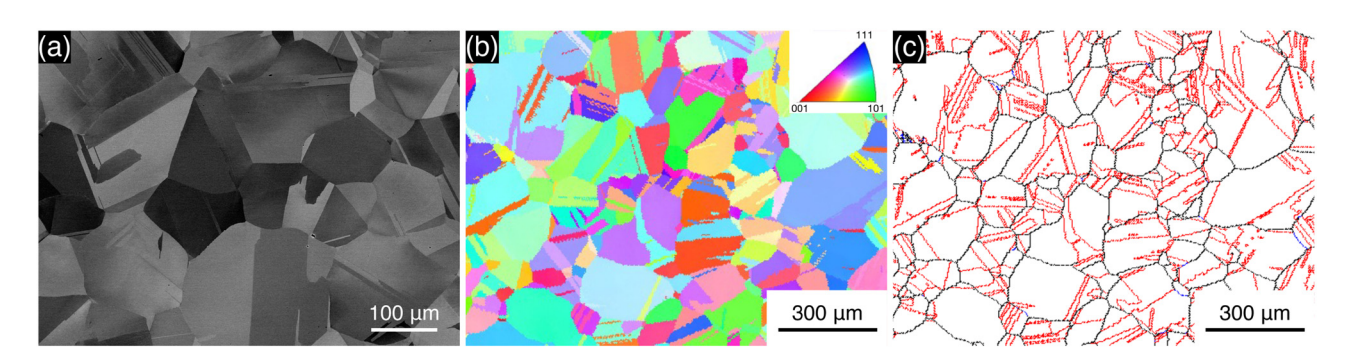


Figure 1: (a) SEM-BSE image, (b) IPF map, and (c) boundary map of the initial microstructure of the Co-28Cr-6Mo-1.5Si alloy substrate prior to immersion tests. In the boundary map, the black, blue, and red lines represent high-angle boundaries (15° $\leq \theta$), low-angle boundaries (2° $\leq \theta < 15^{\circ}$), and annealing twin boundaries, respectively.

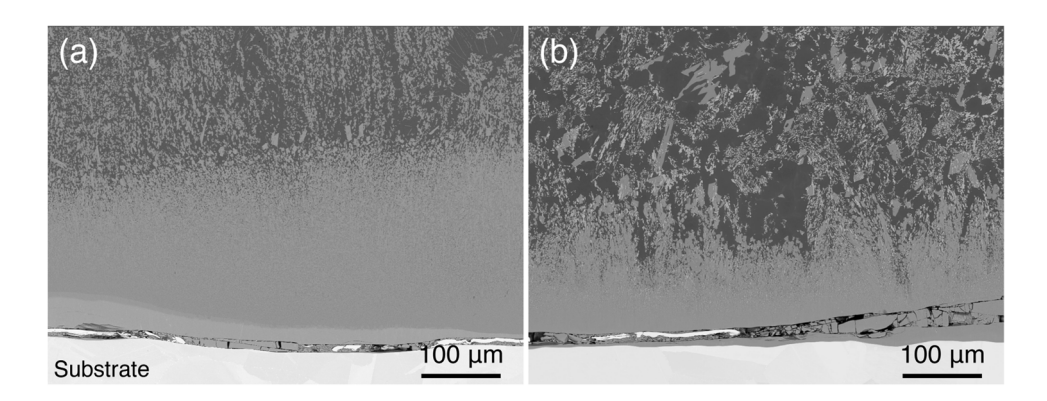


Figure 2: SEM-BSE images for interfaces between the Co-28Cr-6Mo-1.5Si alloy substrate and Al melt: (a) pure Al and (b) ADC12.

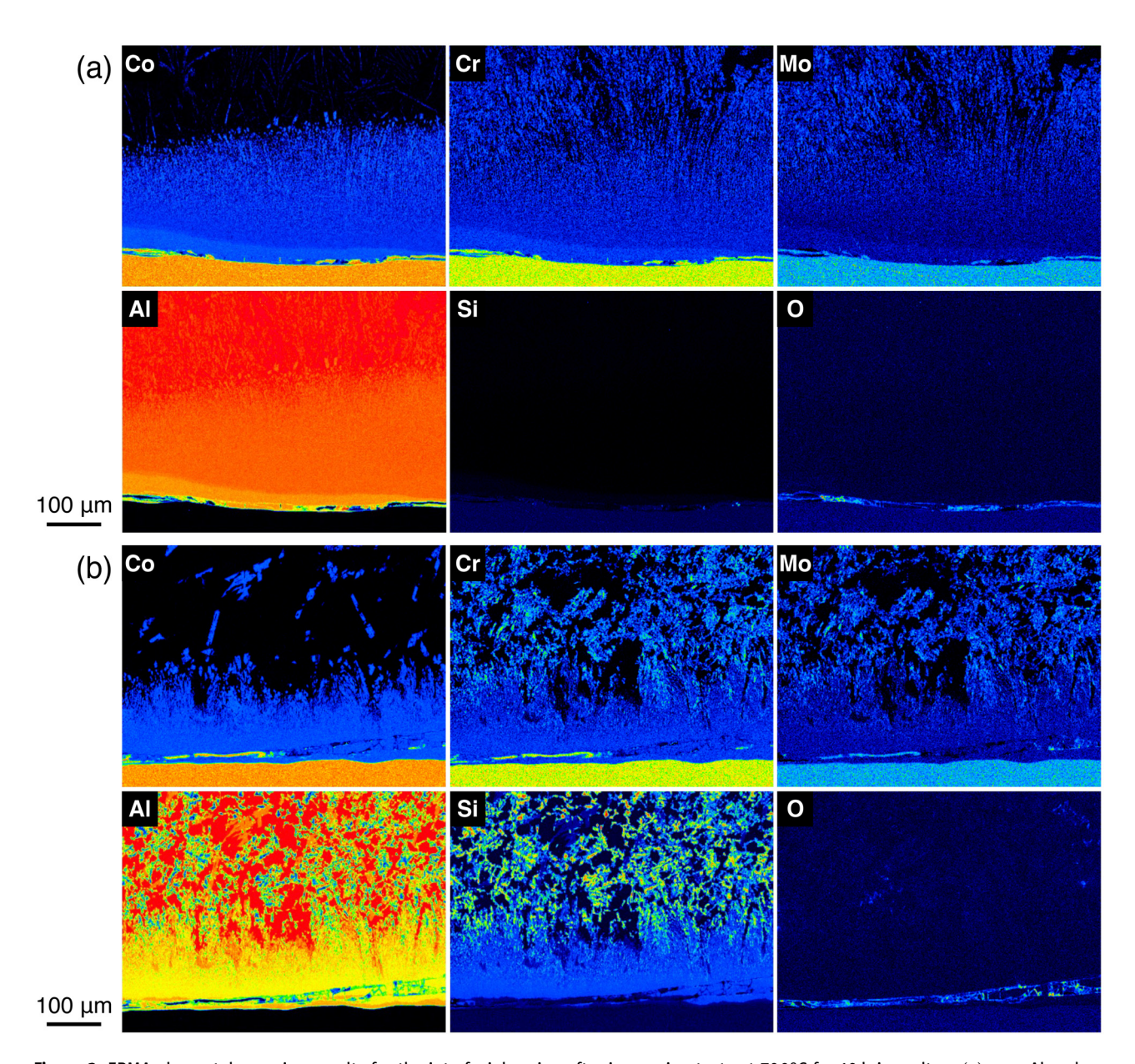


Figure 3: EPMA elemental mapping results for the interfacial region after immersion tests at 700°C for 10 h in molten: (a) pure Al and (b) ADC12.

of the Co-28Cr-6Mo-1.5Si alloy substrate occurs during immersion, causing a contrast in the solidified Al portions. Interfacial layers, which represent cracks, are observed under both the conditions.

Figure 3(a) shows the EPMA elemental mapping results for the interfacial region after the immersion test in pure Al. The results indicate that Co, Cr, and Mo dissolve in the pure Al melt during immersion at 700°C. Co is preferentially located closer to the Co-Cr-Mo alloy substrate. No significant convection was expected during the static immersion tests. Thus, the spatial elemental distribution could be correlated with the diffusion coefficient of Co in

liquid Al, which is slightly higher than that of Cr at 700°C [29], although the solidification process after the immersion test can also affect such distributions. The interfacial region where cracks were observed in Figure 2(a) corresponds to the oxide layer. Similarly, Figure 3(b) clearly shows the dissolution of the Co-Cr-Mo alloy substrate in molten ADC12. The distributions of dissolved Co, Cr, and Mo in the melt are similar to those in the pure Al melt. Notably, the distributions of Cr, Mo, and Si suggest a strong interaction between these elements, and the Si concentration is lower in the vicinity of the Co-Cr-Mo alloy surface.

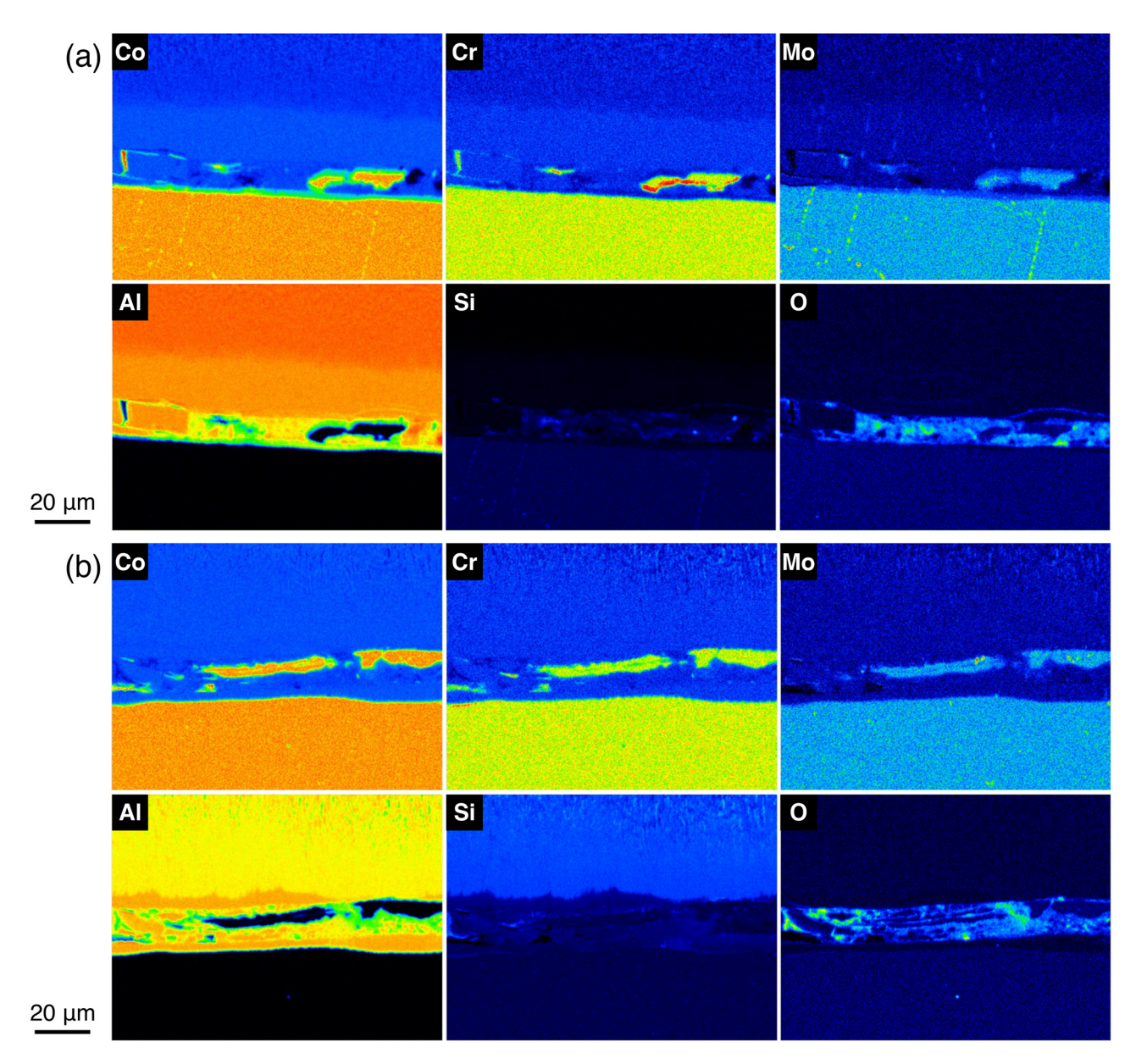


Figure 4: High-magnification EPMA elemental mapping results for the interfacial region after immersion tests at 700°C for 10 h in molten: (a) pure Al and (b) ADC12.

Figure 4 shows high-magnification EPMA elemental maps of the interfacial regions. The Co-Cr-Mo alloy represents Mo-rich σ-phase precipitation that is potentially associated with a partial $y \rightarrow \epsilon$ phase transformation [30]. Detailed EPMA analysis reveals that the Co-Cr-Mo alloy substrate is in direct contact with molten Al, as the Al and O distributions do not overlap, which leads to continuous dissolution. According to the Ellingham diagram, the most favorable oxide among the relevant elements (Co, Cr, Al, and Si) is Al₂O₃. The formation of Al₂O₃ is only observed on the metal Al layer, which does not act as a barrier. Although Si is distributed in the oxide layer and SiO₂ is formed, Si is not homogeneously distributed at the interface. This is true for molten ADC12 despite the higher Si content in the melt (Figure 4(b)). Furthermore, Cr₂O₃, which can act as a barrier against molten Al [19], is not clearly observed on the Co-Cr-Mo alloy surface after immersion. Thus, the dissolution of the Co-Cr-Mo alloys occurs via direct reaction with molten Al. These results are attributable to the low oxygen concentration in the Al and ADC12 used in this study because the solubility of oxygen in Al is extremely small; therefore, it is difficult to form a homogeneous protective oxide layer in molten Al. Moreover, molten Al reduces other oxides, such as CoO, Cr₂O₃, and SiO_2 , to form Al_2O_3 [19].

The results suggest that the reactivity of ADC12 was higher than that of pure Al. Notably, according to the Al-Si binary phase diagram [10], the liquidus temperature of Al decreases from 659.7°C for pure Al to 577°C in the eutectic composition (12.6 wt%). Thus, the test temperature (700°C) relative to the liquidus temperature was higher in ADC12 than that in pure Al, which could have caused corrosion. The addition of Cu (1.88 wt% concentration) in the ADC12 also reduces the liquidus temperature, although its contribution is much less significant than that of the Si because of its lower concentration. The hightemperature characteristics of liquid Al, such as viscosity and wettability with Co-Cr-Mo alloys, require further analysis. Detailed mechanism of the more severe corrosion related to the ADC12 melt would be further investigated. The interfacial reaction reported in this study could improve alloy designs and contribute to applications in thermal storage modules.

4 Conclusions

In this study, the corrosion behavior of Co-28Cr-6Mo-1.5Si alloy in pure molten Al and ADC12 was examined for its potential application in TES. The thickness losses were

evaluated after static immersion tests at 700°C for 10 h, and the interfacial reactions were examined. The main conclusions of this study are summarized as follows:

- The initial microstructure of the Co–28Cr–6Mo–1.5Si alloy after annealing at 1,150°C for 30 min consisted of equiaxed γ grains with no significant texture. The average grain size was approximately 100 μ m.
- The thickness loss of the substrates measured after 10 h of immersion at 700°C was approximately twice as high in the ADC12 melt.
- The interfacial analysis suggested that although the formation of Al₂O₃ and SiO₂ was observed at the interfaces in both the pure Al and ADC12 melt, molten Al was in direct contact with the substrate in both cases. This led to a continuous increase in dissolution as time progressed.

Acknowledgement: The authors acknowledge Issei Narita for technical assistance with EPMA analysis under the GIMRT Program of the Institute for Materials Research, Tohoku University (Proposal No. 202112-CRKEQ-0414).

Funding information: This article is based on results obtained from a project (No. JPNP16002) subsidized by the New Energy and Industrial Technology Development Organization (NEDO).

Author contributions: Kenta Yamanaka: conceptualization, methodology, validation, formal analysis; investigation, resources, data curation, writing – original draft, visualization, project administration, funding acquisition; Manami Mori: investigation, writing – review and editing; Kazuo Yoshida: investigation; Phacharaphon Tunthawiroon: validation, writing – review and editing; Akihiko Chiba: resources, supervision, funding acquisition.

Conflict of interest: The authors state no conflict of interest.

References

- [1] Jones-Albertus, B. Confronting the duck curve: How to address over-generation of solar energy, 2017. https://www.energy.gov/eere/articles/confronting-duck-curve-how-address-overgeneration-solar-energy. accessed December 8, 2022.
- [2] Aneke, M. and M. Wang. Energy storage technologies and real life applications – a state of the art review. Applied Energy, Vol. 179, 2016, pp. 350–377.
- [3] Zalba, B., J. M. Marín, L. F. Cabeza, and H. Mehling. Review on thermal energy storage with phase change: materials, heat

- transfer analysis and applications. Applied Thermal Engineering, Vol. 23, No. 3, 2003, pp. 251-283.
- Shabgard, H., T. L. Bergman, N. Sharifi, and A. Faghri. High [4] temperature latent heat thermal energy storage using heat pipes. International Journal of Heat and Mass Transfer, Vol. 53, 2010, pp. 2979-2988.
- Prieto, C. and L. F. Cabeza. Thermal energy storage (TES) with phase change materials (PCM) in solar power plants (CSP). Concept and plant performance. Applied Energy, Vol. 25415, 2019, id. 113646.
- Kenisarin, M. M. High-temperature phase change materials for thermal energy storage. Renewable and Sustainable Energy Reviews, Vol. 14, No. 3, 2010, pp. 955-970.
- Shamberger, P. J. and N. M. Bruno. Review of metallic phase change materials for high heat flux transient thermal management applications. Applied Energy, Vol. 258, 2020, id. 113955.
- Wang, X., J. Liu, Y. Zhang, H. Di, and Y. Jiang. Experimental research on a kind of novel high temperature phase change storage heater. Energy Conversion and Management, Vol. 47, 2006, pp. 2211-2222.
- Wang, Z., H. Wang, X. Li, D. Wang, Q. Zhang, G. Chen, et al. Aluminum and silicon based phase change materials for high capacity thermal energy storage. Applied Thermal Engineering, Vol. 89, 2015, pp. 204-208.
- [10] Warmuzek, M. Aluminum-silicon casting alloys: atlas of microfractographs, ASM International, Materials Park, OH, USA, 2004.
- [11] Yan, M. and Z. Fan. Review durability of materials in molten aluminum alloys. Journal of Materials Science, Vol. 36, 2001, pp. 285-295.
- [12] Vončina, M., T. Balaško, J. Medved, and A. Nagode. Interface reaction between molten Al99.7 aluminum alloy and various tool steels. Materials, Vol. 14, 2021, id. 7708.
- [13] Sundavist, M. and S. Hogmark. Effects of liquid aluminium on hot-work tool steel. Tribology International, Vol. 26, 1993, pp. 129-134.
- [14] Zhang, J., P. Hosemann, and S. Maloy. Models of liquid metal corrosion. Journal of Nuclear Materials, Vol. 404, No. 1, 2010,
- [15] Sande, J. B., J. R. Coke, and J. Wulff. A transmission electron microscopy study of the mechanisms of strengthening in heattreated Co-Cr-Mo-C alloys. Metallurgical Transactions A, Vol. 7, 1976, pp. 389-397.
- [16] Dobbs, H. S. and J. L. M. Robertson. Heat treatment of cast Co-Cr-Mo for orthopaedic implant use. Journal of Materials Science, Vol. 18, 1983, pp. 391-401.
- [17] Yamanaka, K., M. Mori, S. Kurosu, H. Matsumoto, and A. Chiba. Ultrafine grain refinement of biomedical Co-29Cr-6Mo alloy during conventional hot-compression deformation. Metallurgical and Materials Transactions A, Vol. 40, 2009, pp. 1980-1994.
- [18] Tang, N., Y. P. Li, S. Kurosu, H. Matsumoto, Y. Koizumi, and A. Chiba. Interfacial reactions between molten Al and a

- Co-Cr-Mo alloy with and without oxidation treatment. Corrosion Science, Vol. 5312, 2011, pp. 4324-4326.
- [19] Tunthawiroon, P., Y. Li, and A. Chiba. Influences of alloyed Si on the corrosion resistance of Co-Cr-Mo alloy to molten Al by iso-thermal oxidation in air. Corrosion Science, Vol. 100, 2015, pp. 428-434.
- [20] Tunthawiroon, P., Y. Li, N. Tang, and A. Chiba. Enhancement of corrosion resistance of Fe-Cr-Mo alloy to molten Al by thermal oxidation in air. Corrosion Science, Vol. 77, 2013, pp. 97-102.
- Xu, G., K. Wang, X. Dong, L. Yang, M. Ebrahimi, H. Jiang, et al. Review on corrosion resistance of mild steels in liquid aluminum. Journal of Materials Science & Technology, Vol. 71, 2021, pp. 12-22.
- [22] Long, J., W. Ding, and Y. Yang. Research on the corrosion resistance and mechanism of Fe-Cr-Si alloy in molten aluminum. Corrosion Science, Vol. 201, 2022, id. 110303.
- [23] Yamanaka, K., M. Mori, and A. Chiba. Surface characterisation of Ni-free Co-Cr-W-based dental alloys exposed to high temperature and the effects of silicon addition. Corrosion Science, Vol. 94, 2015, pp. 411-419.
- [24] Tunthawiroon, P., M. Kitiwan, K. Srirussamee, Y. Li, K. Yamanaka, and A. Chiba. Characterization of oxide films on wrought Co-Cr-Mo-xSi alloys exposed to high-temperature oxidation. Corrosion Science, Vol. 191, 2021, id. 109753.
- [25] Yang, X., C. Li, Z. Ye, X. Zhang, M. Zheng, J. Gu, et al. Corrosion behaviors of CoCrWAlx alloys by laser additive manufacturing in molten Al. Corrosion Science, Vol. 193, 2021, id. 109874.
- [26] Liu, M., N. H. S. Tay, S. Bell, M. Belusko, R. Jacob, G. Will, et al. Review on concentrating solar power plants and new developments in high temperature thermal energy storage technologies. Renewable and Sustainable Energy Reviews, Vol. 53, 2016, pp. 1411-1432.
- [27] Sun, J. Q., R. Y. Zhang, Z. P. Liu, G. H. Lu, and . Thermal reliability test of Al-34%Mg-6%Zn alloy as latent heat storage material and corrosion of metal with respect to thermal cycling. Energy Conversion and Management, Vol. 48, 2007, nn. 619-624.
- [28] Yamanaka, K., M. Mori, K. Kuramoto, and A. Chiba. Development of new Co-Cr-W-based biomedical alloys: effects of microalloying and thermomechanical processing on microstructures and mechanical properties. Materials & Design, Vol. 55, 2014, pp. 987-998.
- [29] Du, Y., Y. A. Chang, B., Huang, W. Gong, Z. Jin, H. Xu, et al. Diffusion coefficients of some solutes in fcc and liquid Al: critical evaluation and correlation. Materials Science and Engineering: A, Vol. 363, 2003, pp. 140-151.
- [30] Mori, M., K. Yamanaka, and A. Chiba, Phase decomposition in biomedical Co-29Cr-6Mo-0.2N alloy during isothermal heat treatment at 1073 K. Journal of Alloys and Compounds, Vol. 520, 2014, pp. 411-416.